Plant Physiology and Biochemistry 141 (2019) 206–214

Contents lists available at ScienceDirect

Plant Physiology and Biochemistry

journal homepage: www.elsevier.com/locate/plaphy

Research article

Functional characterization of DiMMS21, a SUMO ligase from *Desmodium intortum*

Xuan Zhou[a], Jinju Du[a], Yiyang Liu[b,c,a], Chengwei Yang[a], Jianbin Lai[a,*]

[a] Guangdong Provincial Key Laboratory of Biotechnology for Plant Development, School of Life Science, South China Normal University, Guangzhou, 510631, China
[b] Biotechnology Research Center, Shandong Academy of Agricultural Sciences; Shandong Provincial Key Laboratory of Crop Genetic Improvement, Ecology and Physiology, Jinan, 250100, China
[c] College of Life Science, Shandong Normal University, Jinan, 250014, China

ARTICLE INFO

Keywords:
Desmodium intortum
MMS21
SUMO ligase
SUMOylation

ABSTRACT

SUMOylation is an important protein modification that regulates the properties of substrate proteins in a variety of cellular processes. SUMOylation is catalyzed via a cascade of enzymes and is usually stimulated by SUMO E3 ligases. However, the molecular functions and regulatory mechanisms of SUMOylation in forage crops are unknown. Here, we isolated and functionally characterized DiMMS21, a homolog of the *Arabidopsis thaliana* SUMO ligase AtMMS21, from the forage legume *Desmodium intortum*. *DiMMS21* is expressed ubiquitously in various *D. intortum* organs and its encoded protein is found in the cytoplasm and nucleus. Bioinformatics analysis indicated that DiMMS21 contains a conserved SP-RING domain that is required for its activity. Biochemical evidence supports the notion that this protein is a functional SUMO ligase. When expressed in an *Arabidopsis mms21* mutant, *DiMMS21* completely rescued the defects in root, leaf, and silique development. The results from cotyledon greening and marker gene expression suggested that *DiMMS21* can only partially complements the role of AtMMS21 in abscisic acid (ABA) responses. In summary, we characterized the molecular features of DiMMS21 and uncovered potential roles of this SUMO ligase in development and ABA responses, increasing our understanding on the function of SUMOylation in forage crops.

1. Introduction

Proteins in eukaryotic cells are regulated by a variety of post-translational modifications, such as methylation, phosphorylation, acetylation, glycosylation, and ubiquitination by ubiquitin and ubiquitin-like proteins during diverse biological processes (Kerscher et al., 2006). Similar to ubiquitin, small ubiquitin-like modifier (SUMO) is a small polypeptide that covalently attaches to the lysine residues of its substrate proteins (Augustine and Vierstra, 2018). Unlike ubiquitin, which is usually involved in protein degradation via the 26S proteasome, SUMO is usually involved in regulating the localization, stability, or activity of different substrates (Hay, 2013). The SUMO conjugation pathway involves a cascade of enzymes including E1 (SUMO-activating enzyme), E2 (SUMO-conjugating enzyme), and usually E3 (SUMO ligase) (Wilkinson and Henley, 2010). Moreover, SUMO can be removed by SUMO proteases for recycling. This contributes to dynamic changes in the modification status of specific substrate proteins (Elrouby, 2017).

In yeast and mammalian cells, SUMOylation is a critical regulator of many cellular processes, such as innate immunity, the cell cycle, DNA repair, chromatin maintenance, and transcriptional control (Seeler and Dejean, 2003). Proteomics approaches have identified many SUMOylation substrates in *Arabidopsis thaliana* (Miller et al., 2010, 2013; Rytz et al., 2018), suggesting that SUMOylation is also a critical in regulation of proteins in plant cells. Detailed functional studies have revealed that SUMOylation is involved in plant development and stress responses (Augustine and Vierstra, 2018). Moreover, the enzymes required for SUMOylation in plant cells are essential for various biological processes. For instance, the depletion of the E1 activating or E2 conjugating enzymes results in embryo lethality in Arabidopsis (Saracco et al., 2007).

Two E3 SUMO ligases, AtSIZ1 and AtMMS21 (also known as HPY2), have been identified in Arabidopsis; these proteins might stimulate the SUMOylation of specific substrates (Miura et al., 2005; Catala et al., 2007; Huang et al., 2009; Ishida et al., 2009). AtSIZ1 primarily participates in signal transduction during responses to environmental changes, such as heat, cold, and phosphate starvation, as well as salicylic acid and abscisic acid (ABA) treatment. Many proteins associated with these pathways are substrates of AtSIZ1 (Castro et al., 2012).

---

[*] Corresponding author.
E-mail address: 20141062@m.scnu.edu.cn (J. Lai).

https://doi.org/10.1016/j.plaphy.2019.06.003
Received 24 January 2019; Received in revised form 2 June 2019; Accepted 3 June 2019
Available online 04 June 2019

AtMMS21 is a functional SUMO ligase with a conserved SP-RING motif that is essential for its enzyme activity. The loss of *AtMMS21* results in developmental defects in roots, leaves, and siliques (Huang et al., 2009; Ishida et al., 2009), likely due to the stimulation of critical components in these developmental processes. For instance, the E2Fa/DPa complex is dissociated by AtMMS21 in the G1/S transition of the cell cycle (Liu et al., 2016). SUMOylation of BRAHMA, a SWI/SNF component required for chromatin remodeling, is also regulated by AtMMS21, in transcriptional control during root development (Zhang et al., 2017a). AtMMS21 interacts with RPT2A, a component of the 26S proteasome, to regulate proteasome activity during development (Yu et al., 2019). In addition, AtMMS21 functions as a component of the SMC5/6 complex, which is involved in homologous recombination during DNA repair and meiosis (Xu et al., 2013; Liu et al., 2014; Yuan et al., 2014). AtMMS21 also takes part in the regulation of ABA-dependent drought responses (Zhang et al., 2013).

In contrast to SIZ1, which has been functionally characterized in several other plant species, such as rice (*Oryza sativa*), tomato (*Solanum lycopersicum*), soybean (*Glycine max*), apple (*Malus* sp.), and *Dendrobium* (Park et al., 2010; Liu et al., 2015; Zhang et al., 2016, 2017b; Cai et al., 2017), the roles of MMS21 homologs in other plants have not yet been reported. Here, we performed functional characterization of DiMMS21, an MMS21 homolog from *Desmodium intortum* (Debela et al., 2012). *D. intortum*, a large perennial legume found in tropical and subtropical regions, is an important forage crop with high feeding and commercial value due to its rapid growth, high yields, and high nutritional composition (Nurfeta et al., 2009). This legume has a well-developed root system, which is critical for its rapid growth and nitrogen fixation (Nurfeta, 2010). However, abiotic stresses such as low temperature and drought limit the distribution of this forage crop (Midega et al., 2017). AtMMS21 is involved in root development and stress responses in Arabidopsis; therefore, we performed functional analysis of the homolog of AtMMS21 in *D. intortum*. We identified DiMMS21, analyzed its sequence, and compared it to MMS21 homologs from other species. In addition, we investigated the expression patterns of *DiMMS21* in various *D. intortum* organs. Finally, we introduced *DiMMS21* into the *AtMMS21* mutant and analyzed its function in root, leaf and silique development, as well as in ABA sensitivity. Our findings expand our understanding of the roles of MMS21 in plants and provide hints about the role of SUMOylation in regulating development and stress responses in forage legumes.

2. Materials and methods

2.1. Plant materials and growth conditions

The seeds of *D. intortum* were obtained from the Guangdong Provincial Key Laboratory of Biotechnology for plant development research at the School of Life Science, South China Normal University. Plump seeds were sterilized and planted in a well-prepped seedbed plastic boxes filled with soil substrates, following the establishment and management for conservation plantings described in the USDA NRCS Hoolehua Plant Materials Center, Hoolehua, Hawaii. The boxes were placed in a climate control cabinet with the temperature set at 25 °C; a 10-h light/14-h dark photoperiod, and a humidity of 60%. *Arabidopsis thaliana* plants (Columbia-0 wild type and *mms21-1* (Huang et al., 2009) from ABRC) were grown in conditions at 21 °C with 16-h-light/8-h-dark cycles, photoperiod, and humidity of 40%. Seeds were surface sterilized and sown on half-strength Murashige and Skoog (MS) medium containing 1% sucrose and 0.8% agar.

2.2. Isolation and detection of the full-length CDS of DiMMS21

Total RNA from *D. intortum* was extracted using the TRIZOL reagent (Tiangen) following the manufacturer's instructions. Samples were treated with DNase (Promega) to eliminate genomic DNA contamination. DNA-free RNA was used for reverse transcription by the PrimeScript™ RT reagent Kit (Takara) and sent for further RNA-seq analysis. Based on the gene annotations of the de novo sequences from RNA-Seq, a cDNA encoding a potential MMS21 homolog in *D. intortum* (DiMMS21) was chosen for further study. Its sequence similarity with MMS21 proteins in other species was confirmed by BLASTP using the deduced amino acid sequence from the cDNA. The full-length CDS of *DiMMS21*, was amplified via RT- PCR using the primers *pCanG-DiMMS21*-F/R, and cloned into the *pCanG* vector under control of a *35S* promoter using *Aat*II and *Sma*I. The CDS information of *DiMMS21* in the construct was verified via sequencing. The sequence information of the primers used in this study is included in Table S1.

2.3. Bioinformatics analysis of DiMMS21

The CDS of *DiMMS21* was translated into protein sequence for bioinformatics analysis. The theoretical PI (isoelectric point) and MW (molecular weight) of DiMMS21 was predicted via the online program pI/MW from Expasy (https://web.expasy.org/compute_pi/)(Gasteiger et al., 2003). The phylogenetic tree was constructed using the amino acid sequences of MMS21 homologs from different species by MEGA5.1 with 1000 bootstrap tests by the Maximum Likelihood method (Tamura et al., 2011). Alignment of protein sequence among DiMMS21 and other homologs were performed via the Clustal software (http://www.clustal.org/) (Sievers et al., 2011). Predicted molecular modeling of the DiMMS21 structure was built on the phyre2 online server (http://www.sbg.bio.ic.ac.uk/phyre2/) (Kelley et al., 2015).

2.4. Subcellular localization of DiMMS21

The CDS of *DiMMS21* was amplified by RT-PCR, using the primers *pYFP-DiMMS21*-F/R, and cloned into an YFP expression vector based on *pBluescript* (Liu et al., 2016), using *Bam*HI and *Nco*I. The empty vector with YFP was used as a control. The plasmids were transformed into Arabidopsis protoplasts for transient expression, according to the protocol from the Sheen's laboratory (Yoo et al., 2007). 48 h after transformation, the YFP fluorescence was detected under a Zeiss LSM 710 laser microscope with 514 nm for excitation and 530–600 nm for emission. The signals from chlorophyll auto-fluorescence were also recorded.

2.5. SUMOylation assay

To detect the auto-SUMOylation activity of DiMMS21, the CDS of *DiMMS21* without the stop codon was amplified by RT-PCR using the primers *pCDF-DiMMS21*-F/R (the coding sequence of a FLAG tag was included in the *pCDF-DiMMS21-R* primer for generation of the DiMMS21-FLAG protein), then was cloned into the *pCDFDuet-1* vector using *Bam*HI and *Sal*I. The plasmid was transformed into bacteria strain *BL21 (DE3)* carrying *pET28-SAE1a-His-AtSAE2* (E1) (Budhiraja et al., 2009) and *pACYCDuet-1-SCE1-SUMO1(GG)* (E2 and SUMO1) (The plasmids were transformed sequentially) for detection of SUMO conjugation (Okada et al., 2009). The transformed cells were cultured in LB medium to an OD_{600} of 0.5 and induced for protein expression by 0.2 mM IPTG (final concentration). After incubation for 12 h at 25 °C, cells were harvested, mixed with 4 × SDS sample buffer and boiled for 5 min for regular SDS-PAGE. After electrophoresis, proteins were transferred onto a PVDF membrane (Immobilon, USA). The membrane was incubated sequentially with 5% non-fat milk in PBST for 30 min, the rabbit anti-FLAG antibody (Sigma) for 1 h, and the anti-rabbit HRP-linked antibody (Cell Signaling Technology) for 1 h. The signals were visualized by chemiluminescence using the ECL plus kit (Cwbio, China) according to the manufacturer's instructions.

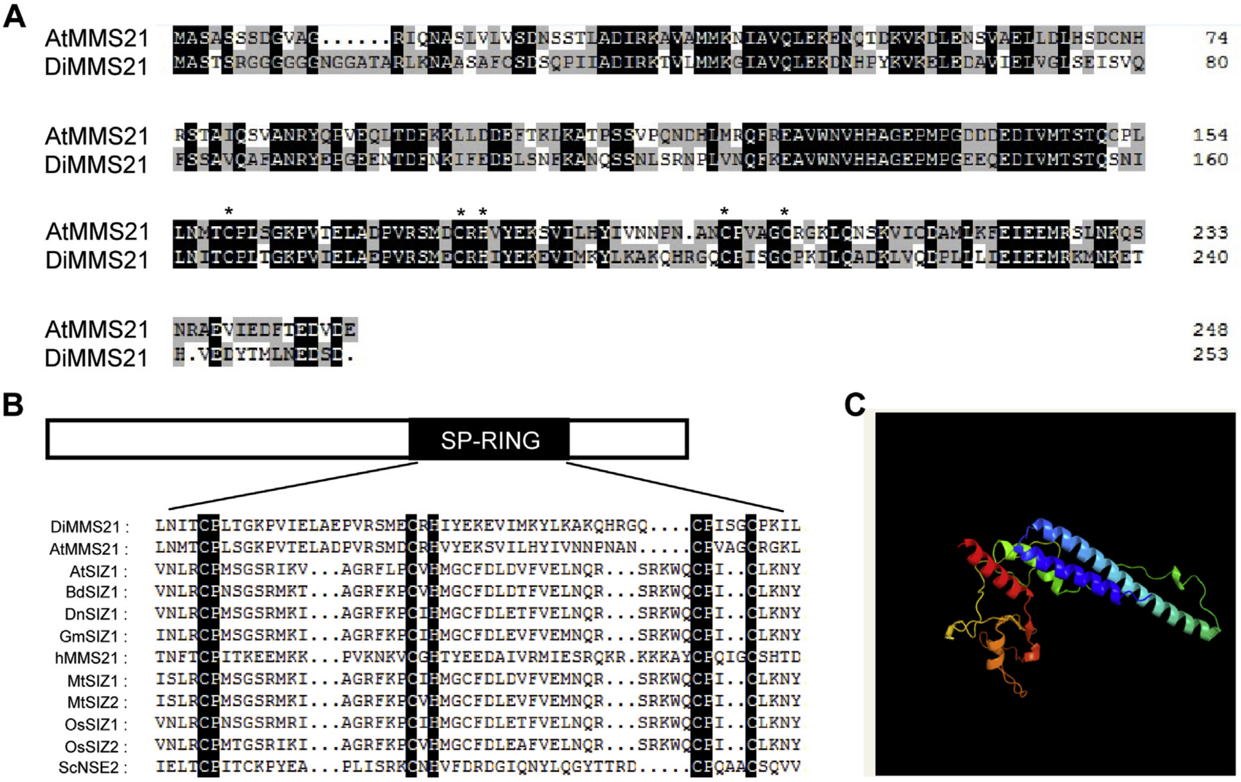

Fig. 1. Molecular analysis of DiMMS21 based on bioinformatics. (A) Amino acid sequence alignment of DiMMS21 and AtMMS21. The alignment was performed using Clustal software.*The conserved cystine/histidine residues in the SP-RING domain. (B) Alignment of the amino acid residues in the SP-RING domain. The MMS21 and SIZ1 homologs from various species were used in the analysis. (C) Predicted molecular model of the DiMMS21 protein structure.

2.6. Generation of the DiMMS21 complemented plants

The *pCanG-DiMMS21* plasmid was introduced into *Agrobacterium tumefaciens EHA105* for further transformation into the *Arabidopsis thaliana*, wild type or *mms21-1*, via the floral dip method (Clough and Bent, 1998). The transformed plants were selected on the MS medium supplemented with kanamycin. The transcript level of T3 homozygous plants was verified via RT-PCR. The representative lines with overexpression of *DiMMS21* were used for phenotype analysis.

2.7. ABA treatment

Seeds were sown in the plates containing MS medium without or with different concentrations of ABA. Plates were exposed at 4 °C in the dark for 2 d and moved to 22 °C with a 16 h light/8 h dark cycle. The percentage of seed germination was scored at indicated times. Germination was defined as an obvious emergence of the radicle through the seed coat. Cotyledon greening is defined as obvious cotyledon expansion and greening.

2.8. Measurement of transcript levels

To detect the expression profile of *DiMMS21*, RNA from different organs of *Desmodium intortum* was extracted and the genomic DNA was removed following the methods described above. A similar amount of RNA from each sample was used for reverse transcription, then the cDNA was used for semi-quantitative PCR using the primers *RT-DiMMS21*-F/R. The relative levels of signals were analyzed by ImageJ. To detect the expression levels of *DiMMS21* in the transgenic Arabidopsis plants, the procedures of semi-quantitative RT-PCR were similar and *ACTIN1* was used as an internal control (Yang et al., 2011).

To measure the transcript levels of ABA responsive genes, different genotypes of 7-d-old plants were transferred to 1/2 MS liquid mediums with 10 μM ABA for 0, 3 or 6 h, then RNA was extracted using the Plant RNAprep Pure Kit (Tiangen) with DNaseI (Promega) treatment following the manufacturer's instructions and subjected to reverse transcription using a PrimeScript RT Reagent Kit (Takara). RT-qPCR was then carried out using SYBR Premix Ex Taq (Takara) in a Bio-Rad CFX 96 system (C1000 Thermal Cycler) and detected by Bio-Rad CFX Manager software (Bio-Rad). *ACTIN2* was used as an internal control (Zhang et al., 2017a).

2.9. Data analysis

For measurement of root length, the data are mean ± SD from 30 seedlings for each genotype in three independent experiments. For comparison of root meristem cell numbers, the data are mean ± SD from 10 roots for each genotype. For analysis of the leaf area (the 8th rosette leaf, calculated by ImageJ) and silique, the data are mean ± SD from 10 samples for each genotype in three independent experiments. For detection of ABA sensitivity, the data are mean ± SD from three independent experiments (at least 50 seeds for each genotype were used in every experiment). The significant difference was analyzed by the two-tailed Student's *t*-test. ***$p < 0.001$, **$p < 0.01$, *$p < 0.05$, n.s. (no significance): $p > 0.05$.

3. Results

3.1. Isolation and molecular analysis of DiMMS21

To obtain the transcript information of *D. intortum*, its total RNA was extracted for RNA-seq analysis. Based on the gene annotations in the RNA-seq data, a cDNA encoding a potential MMS21 homolog in *D. intortum* (named as DiMMS21) was chosen for further study. We obtained the coding sequence (CDS) of *DiMMS21*by RT-PCR. The complete CDS of *DiMMS21* is 762 bp long, encoding a predicted protein with 253

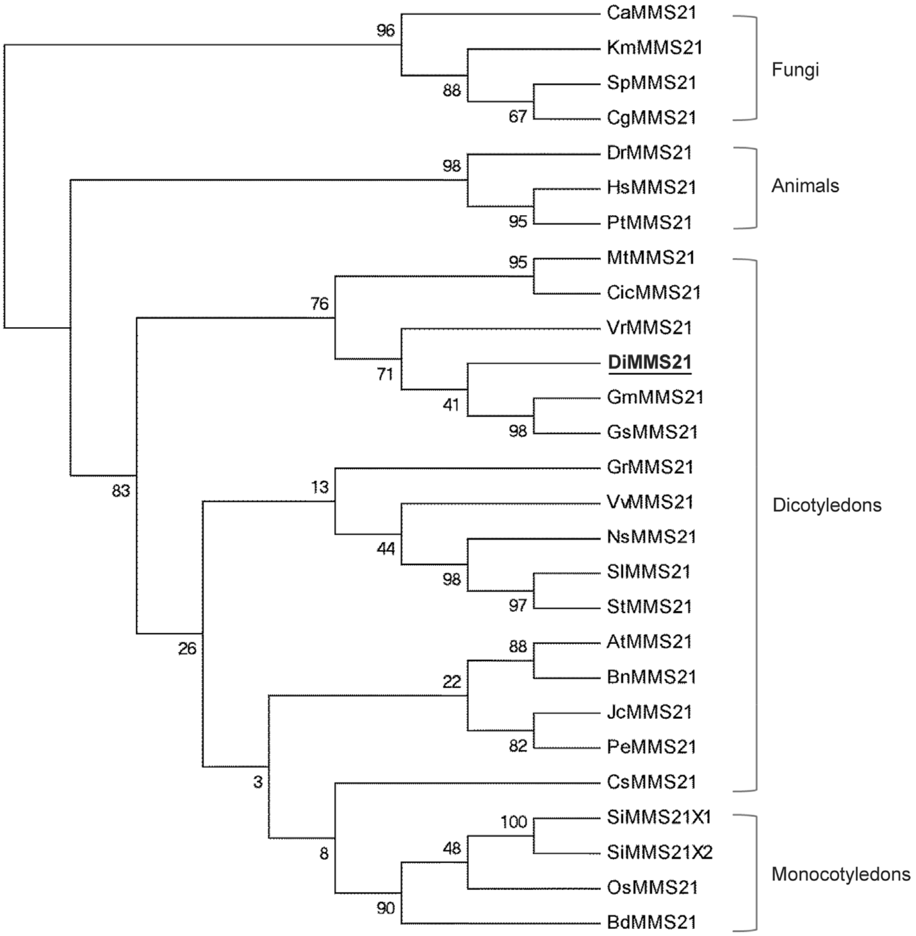

Fig. 2. Phylogenetic analysis of MMS21 proteins from *D. intortum* and other species. The species are *Candida albicans* (Ca), *Kluyveromyces marxianus* (Km), *Saccharomyces cerevisiae* (Sp), *Candida glabrata* (Cg), *Danio rerio* (Dr), *Homo sapiens* (Hs), *Pan troglodytes* (Pt), *Medicago truncatula* (Mt), *Cicer arietinum* (Cic), *Vigna radiata* (Vr), *Desmodium intortum* (Di), *Glycine* max (Gm), *Glycine soja* (Gs), *Gossypium raimondii* (Gr), *Vitis vinifera* (Vv), *Nicotiana sylvestris* (Ns), *Solanum lycopersicum* (Sl), *Solanum tuberosum* (St), *Arabidopsis thaliana* (At), *Brassica napus* (Bn), *Jatropha curcas* (Jc), *Populus euphratica* (Pe), *Cucumis sativus* (Cs), *Setaria italic* (Si), *Oryza sativa* (Os), and *Brachypodium distachyon* (Bd). SiMMS21X1/X2 are two isoforms of SiMMS21. The complete protein sequences were used to construct the phylogenetic tree using the Maximum Likelihood method with MEGA software. The numbers at the nodes indicate the bootstrap values.

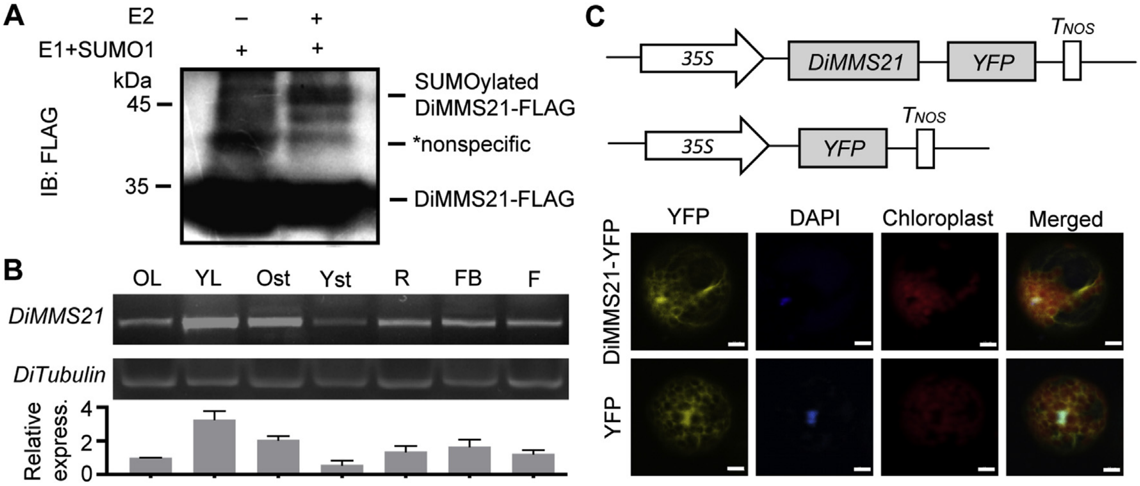

Fig. 3. The SUMO ligase activity, organ-specific expression pattern, and subcellular localization of DiMMS21. (A) Auto-SUMOylation of DiMMS21 was measured in a reconstituted SUMOylation system in *E. coli*. In the presence of E1 and SUMO1, unconjugated and SUMO-conjugated FLAG-tagged DiMMS21 were detected by an anti-FLAG antibody in both the presence and absence of E2. *nonspecific signals. (B) The expression patterns of *DiMMS21*. RT-PCR analysis of *DiMMS21* transcripts in various *D. intortum* organs. *DiTubulin* was used as an internal control. OL, old leaves; YL, young leaves; Ost, old stems; Yst, young stems; R, roots; FB, flower buds; F, flowers. The image is a representative of three experiments. The relative expression data (*DiMMS21/DiTubulin*) are mean ± SD from quantifications via ImageJ. (C) Subcellular localization of DiMMS21-YFP. The constructs are shown in the top panel. Empty vector with YFP was used as a control. The signals were detected using confocal microscopy 24 h after protoplast transformation. DAPI was used for nucleus labeling. The signals from YFP (yellow), DAPI (blue), chloroplast (red), and merged images are shown. Bar = 10 μm. (For interpretation of the references to colour in this figure legend, the reader is referred to the Web version of this article.)

amino acid residues. Information about the CDS and deduced protein sequence of DiMMS21 is provided in Table S2. Its protein sequence similarity with MMS21 proteins from other species was confirmed by BLASTP using the deduced amino acid sequence from the cDNA. The predicted molecular weight of DiMMS21 is 28 kDa, and the predicted PI is 5.1.

Sequence alignment indicated that DiMMS21 and AtMMS21 share 53% amino acid identity (Fig. 1A). The enzyme activity of MMS21 relies on the SP-RING motif, a five-cysteine/histidine residue region required for Zn^{2+} binding, and the residues in this region are highly conserved between DiMMS21 and AtMMS21. The essential residues in the SP-RING domain are also similar to those of SIZ1 proteins in various species (Fig. 1B). Molecular modeling of DiMMS21 suggested that this protein consists of several helices (Fig. 1C).

In addition, we performed phylogenetic analysis using the predicted MMS21 protein sequences of several species from GenBank (Fig. 2). The phylogenetic tree is divided into four clades, including monocotyledons, dicotyledons, fungi, and animal species. The protein sequence of DiMMS21 is similar to that of MMS21 homologs from other legume species, such as *Glycine* max (Gm) and *Glycine soja* (Gs), in the dicotyledon group (Fig. 2). Our sequence and motif similarity analyses support the notion that DiMMS21 is a conserved SUMO ligase.

3.2. SUMO ligase activity, organ-specific expression, and subcellular localization of DiMMS21

Because auto-SUMOylation is important for SUMO ligases in further enhancement of the reaction on protein substrates, we fused DiMMS21 with a FLAG tag and expressed it in a reconstituted SUMOylation system in bacteria (expressing E1, E2 and SUMO1; the bacteria expressing E1 and SUMO1 was used as a negative control) to analyze its auto-SUMOylation activity. In the presence of E1 and E2, the SUMO1 molecules were covalently attached to DiMMS21, resulting in a shift in protein size, as revealed by SDS-PAGE (Fig. 3A), similar to the results from AtMMS21 (Huang et al., 2009; Ishida et al., 2009). This biochemical evidence supports the notion that DiMMS21 is a functional SUMO ligase, although its catalytic activity needs to be confirmed by enhancing SUMOylation of substrates in the further experiments.

In Arabidopsis, *AtMMS21* is expressed in all organs (Huang et al., 2009; Ishida et al., 2009). Therefore, we investigated the expression patterns of *DiMMS21* in various *D. intortum* organs. Semiquantitative RT-PCR indicated that *DiMMS21* was expressed in all organs, including roots, stems, leaves, and flowers. *DiMMS21* transcript levels were highest in young leaves and old stems (Fig. 3B).

Given that SUMOylation primarily occurs in the nucleus and cytoplasm, we examined the subcellular localization of DiMMS21 by fusing *DiMMS21* with *YFP* and expressing this construct in protoplasts. The fusion protein localized to both the nucleus and cytoplasm (Fig. 3C), a pattern similar to that of AtMMS21 (Huang et al., 2009).

3.3. DiMMS21 rescues the developmental defects of the AtMMS21 mutant

Because a transformation system has not yet been established for *D. intortum*, we performed functional analysis of DiMMS21 in Arabidopsis. We cloned the CDS of *DiMMS21* into a plasmid under the control of the *35S* promoter and transferred it into wild-type and *AtMMS21* mutant (*mms21-1*) Arabidopsis. Various transgenic plants overexpressing *DiMMS21* were obtained; representative lines with the proper expression levels were used for functional characterization (Fig. 4A).

Given that *mms21-1* has defects in root development, we measured the root lengths of the complemented plants. The short root phenotype of *mms21-1* was rescued by transformation with *DiMMS21* in seedlings during different seedling developmental stages (Fig. 4B and 4C). The defective root development of *mms21-1* results from a disordered root meristem region (Xu et al., 2013). Indeed, our microscopy analysis indicated that meristem size in *mms21-1* was completely recovered by the overexpression of *DiMMS21* (Fig. 4D and 4E). Because propidium iodide (PI) is used as a marker for dead cells that have a loss of membrane integrity (Truernit and Haseloff, 2008), the results of PI staining indicated that the level of cell death in the root meristem was also dramatically reduced in the complemented plants (Fig. 4D).

We previously demonstrated that AtMMS21 plays roles in regulating leaf and silique development (Huang et al., 2009). Therefore, we analyzed the phenotypes of the complemented plants at several different developmental stages in detail. The leaves were smaller in *mms21-1* than in the wild type, but this defect was completely rescued by *DiMMS21* (Fig. 5A, D). Similarly, the short siliques and dwarf phenotype were also recovered in the complemented plants (Fig. 5B–D). Collectively, these results indicated that DiMMS21 can replace the functions of AtMMS21 in root, leaf, and silique development.

3.4. DiMMS21 partially complements the function of AtMMS21 in ABA responses

Given that *mms21-1* is more sensitive to ABA than the wild type (Zhang et al., 2013), we also compared the ABA sensitivity of *mms21-1* plants with or without *DiMMS21* expression. We plated seeds on medium containing 0, 0.2, 0.5, or 1 μM of ABA and measured the germination percentage and cotyledon greening percentage.

Since there were only small differences in the germination percentages of wild-type versus *mms21-1* seeds under ABA treatment, we focused on the percentage of cotyledon greening in these lines. Compared to the wild type, the cotyledon greening percentage of *mms21-1* was dramatically reduced under ABA treatment. When *DiMMS21* was expressed in the *mms21-1* mutant, the cotyledon greening rate was partially but not completely recovered (Fig. 6). Therefore, DiMMS21 may also be involved in regulating ABA signal transduction, but its molecular role in this process might differ from that of AtMMS21.

To reveal the reason why *DiMMS21* can only partially complement the function of AtMMS21 in ABA responses, the transcript levels of several ABA responsive genes, including *ABI3*, *ABI5*, *RD29B* and *RAB18* (Zhang et al., 2013), were detected. The 7-d-old seedlings were treated with 10 μM ABA for 0, 3 or 6 h, then total RNA was extracted for quantitative RT-PCR. During the ABA treatment, these marker genes were upregulated in all plants with different genotypes. Similar to the previous study (Zhang et al., 2013), following the treatment with ABA, the transcript levels of these genes were higher in the *mms21-1* mutant than those in the wild type (Fig. 7). Overexpression of *DiMMS21* partially repressed the misexpression of these genes in *mms21-1*. Generally, overexpression of *DiMMS21* did not suppress the increasing transcript levels of these genes in the *mms21-1* mutant with 3-h ABA treatment, but inhibited additional increasing of these genes with 6-h ABA treatment (Fig. 7). These quantitative transcript data supported the notion that *DiMMS21* can not completely complement the roles of AtMMS21 in regulating the ABA signaling pathway.

4. Discussion

SUMOylation plays important roles in regulating a number of cellular processes in plants, including development and stress responses (Park and Yun, 2013), but its function in forage crops is unclear. Here, we characterized the molecular role of the SUMO ligase, DiMMS21, from the forage legume *D. intortum*. *DiMMS21* is ubiquitously expressed in a variety of organs in *D. intortum*, suggesting it functions during various stages in this plant. AtMMS21 enhances SUMOylation of proteins including DPa, BRM and RPT2a for maintenance of normal development (Liu et al., 2016; Zhang et al., 2017a; Yu et al., 2019). Interestingly, AtMMS21 is co-localized with these protein substrates in nucleus and/or cytoplasm, supporting that SUMOylation primarily occurs in these subcellular areas. Similar to AtMMS21 (Huang et al., 2009), DiMMS21 is found in both the nucleus and cytoplasm, consistent with its function in this process.

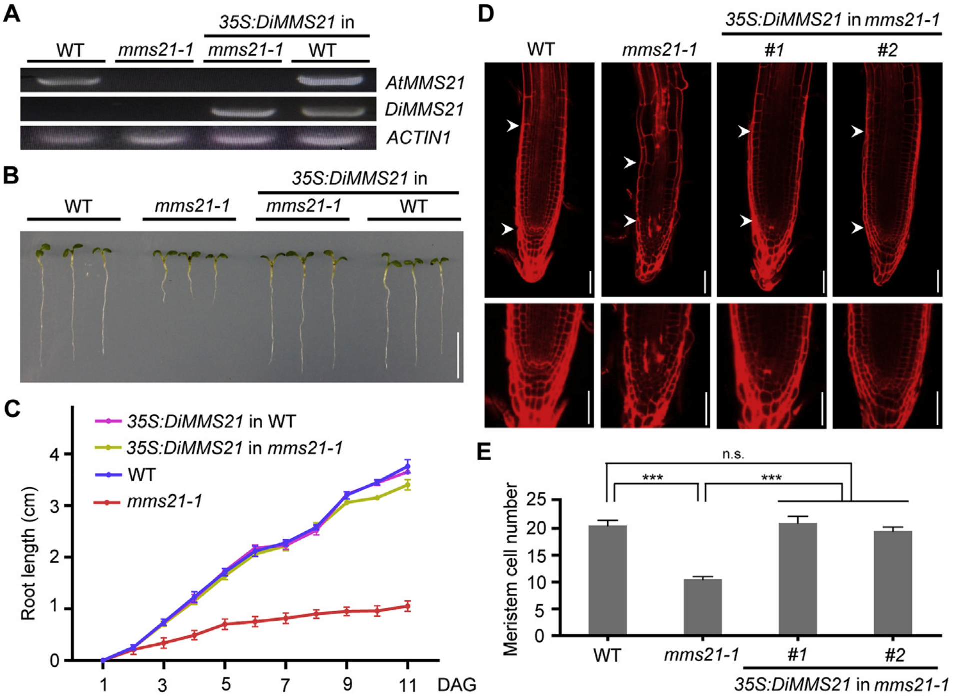

Fig. 4. ***DiMMS21*** **rescues the defective root development of the** ***AtMMS21*** **mutant.** (A) Expression levels of *DiMMS21* and *AtMMS21* in wild-type, *mms21-1* and *DiMMS21/mms21-1*. The transcript levels were measured using RT-PCR. *ACTIN1* was used as an internal control (Yang et al., 2011). (B) Comparison of root length among wild-type and *mms21-1* plants with or without *DiMMS21* expression. The photograph was taken 7 days after germination. Bar = 1 cm. (C) Root length at different time points. DAG, days after germination. The data are mean ± SD from 30 seedlings for each genotype in three experiments. (D) Root meristem regions of wild-type, *mms21-1*, and *DiMMS21 mms21-1* seedlings. The roots of 7-day-old seedlings were stained with 10 μg/mL PI for 1 min and mounted in water for confocal microscopy with the excitation/emission wavelengths: 561 nm/591–635 nm for PI. The meristem regions are indicated by arrowheads. Enlarged images of the quiescent centers are shown in the bottom panel. Dead cells are stained red by PI, resulted from losses of membrane integrity. Bar = 50 μm. (E) Statistical analysis of cell number in the indicated meristems. The data are mean ± SD from 10 seedlings. $^{***}p < 0.001$; n.s. (no significance): $p > 0.05$; Student's *t*-test. (For interpretation of the references to colour in this figure legend, the reader is referred to the Web version of this article.)

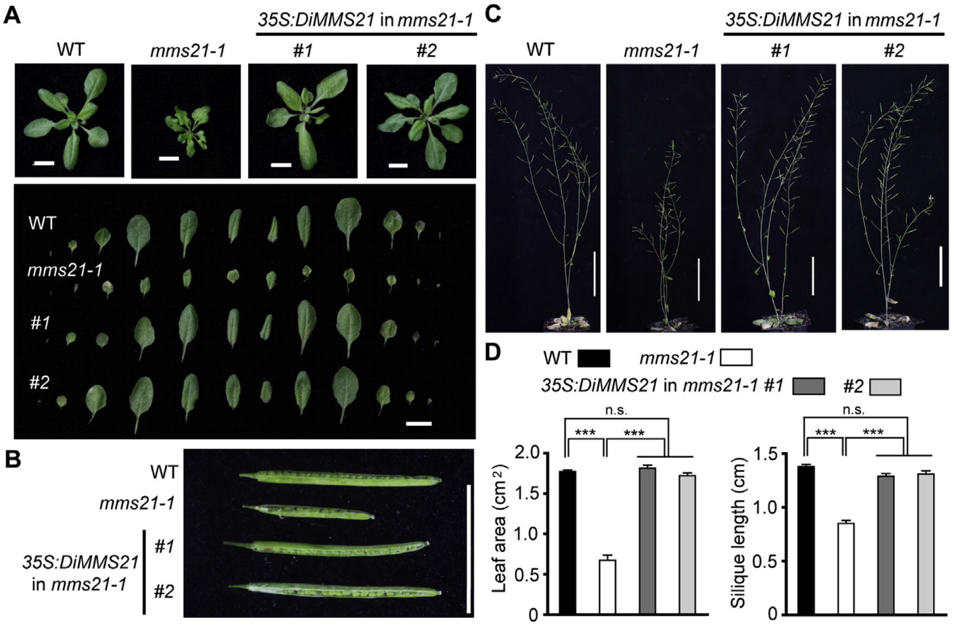

Fig. 5. ***DiMMS21*** **complements the leaf and silique developmental defects of the** ***AtMMS21*** **mutant.** (A) The phenotypes of 3-week-old wild-type, *mms21-1*, and complemented plants. Photographs of whole plants are shown in the top panel, and the detached leaves are shown in the bottom panel. Bar = 1 cm. (B) Siliques from the indicated plants. Bar = 1 cm. (C) The phenotypes of 6-week-old plants. Bar = 5 cm. (D) Statistical analysis of the area of the 8th rosette leaves of 3-week-old plants and silique length of 6-week-old plants. The data are mean ± SD from 10 samples. $^{***}p < 0.001$; n.s. (no significance): $p > 0.05$; Student's *t*-test.

The SUMO ligase MMS21 is conserved among species. Indeed, our alignment analysis showed that the amino acid sequence of DiMMS21 shares high identity with that of AtMMS21, suggesting they might share conserved functions. Phylogenetic analysis supported the evolutionary relationship between DiMMS21 and its homologs in other species. The characteristics of DiMMS21 are closest to those of MMS21 proteins in other dicotyledons, indicating that its protein structure was conserved during evolution. Although the entire protein sequence of DiMMS21 is similar to that of AtMMS21, the most highly conserved region is the SP-RING domain (Duan et al., 2009), which is essential for the SUMOylation reaction. Several critical residues in this region are identical to those of SIZ1 proteins (Ishida et al., 2012), suggesting that DiMMS21 is a functional SUMO ligase; this notion is supported by biochemical evidence from an auto-SUMOylation assay.

SUMOylation is important for many biological processes in plant cells, and many components of the SUMOylation machinery, are essential in plant development and stress responses (Murtas et al., 2003; Miura et al., 2010; van den Burg et al., 2010; Castro et al., 2018). MMS21 is a SUMO ligase that might mediate the SUMOylation of distinct protein substrates in different biological processes. Previous studies showed that depletion of *AtMMS21* in Arabidopsis results in developmental defects (Huang et al., 2009; Ishida et al., 2009; Xu et al., 2013; Liu et al., 2014), as well as hypersensitivity to ABA (Zhang et al., 2013). The developmental defects of the *AtMMS21* mutant, including

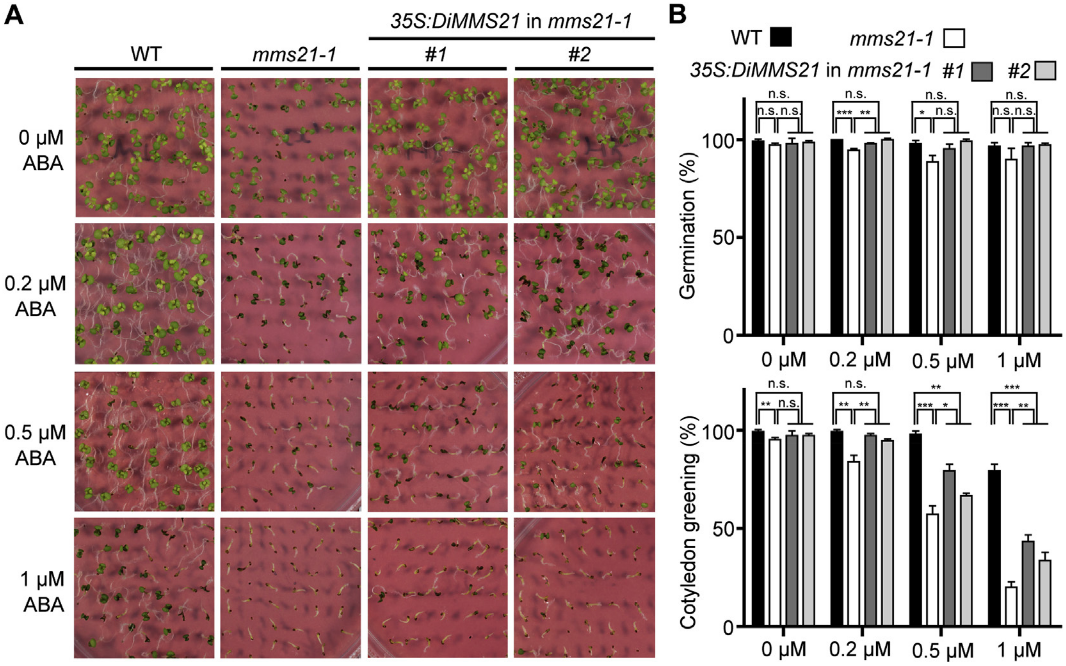

Fig. 6. The effect of *DiMMS21* on ABA sensitivity in the *AtMMS21* mutant. (A) Seeds were stratified on medium containing 0, 0.2, 0.5, or 1 μM ABA. The photographs were taken 10 days after stratification. (B) Germination percentages and cotyledon greening percentages of the lines shown in A. The data are mean ± SD from three independent experiments. ***$p < 0.001$; **$p < 0.01$; *$p < 0.05$; n.s. (no significance): $p > 0.05$; Student's *t*-test.

short roots, small root meristem regions, dwarfism, and short siliques, were completely recovered via overexpression of *DiMMS21*. AtMMS21 enhances SUMO conjugation to DPa, BRM, and RPT2a during development (Liu et al., 2016; Zhang et al., 2017a; Yu et al., 2019). Since these substrates are also conserved among species, it is highly likely that DiMMS21 also helps regulate the activity of their homologs in *D. intortum*.

However, the defect of green cotyledon emergence of the *AtMMS21* mutant in response to ABA was only partially rescued by *DiMMS21* overexpression. Because seed germination and cotyledon greening are two independent processes (Castro et al., 2015), the result also suggests SUMOylation mediated by MMS21 may be more important for post-germination development under ABA treatment. The quantitative RT-PCR data indicated that the transcript levels of the ABA responsive genes, such as *ABI3*, *ABI5*, *RD29B* and *RAB18*, are upregulated in the *AtMMS21* mutant (Zhang et al., 2013), but the increase of these transcript can only be partially suppressed by overexpression of *DiMMS21* (Fig. 7), supporting the notion from cotyledon greening analysis. Interestingly, similar to MMS21, SIZ1 also plays a role in regulation of the ABA responsive genes (Miura et al., 2009), suggesting an interplay between different components in the SUMOylation pathway during ABA signaling transduction. The substrates of AtMMS21 in the ABA signaling pathway have not yet been identified. Therefore, it would be useful to compare the substrate difference between DiMMS21 and AtMMS21 in ABA responses in the future.

D. intortum is used as a forage crop in tropical and subtropical

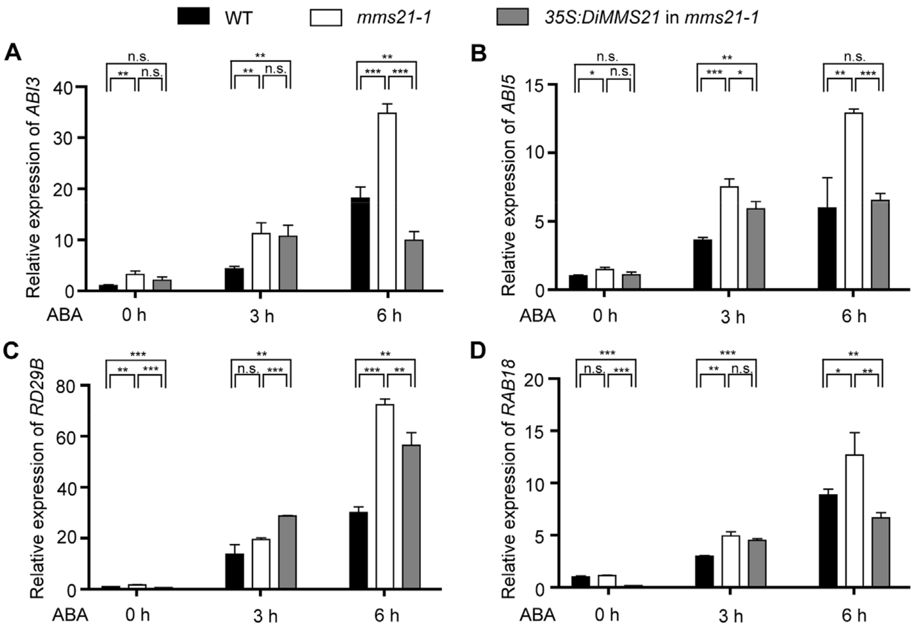

Fig. 7. The effect of *DiMMS21* on the transcript levels of ABA responsive genes in the *AtMMS21* mutant. 7-d-old seedlings of wild type, *mms21-1* and *DiMMS21/mms21-1* were treated with 10 μM ABA for 0, 3 or 6 h. RNA was extracted for quantitative RT-PCR. *ACTIN2* was used as an internal control (Zhang et al., 2017a). The transcript level of each gene in the wild type for 0-h ABA treatment is set to 1, respectively. The relative transcript levels of *ABI3* (A), *ABI5* (B), *RD29B* (C) and *RAB18* (D) are shown. The data are mean ± SD from three experiments. ***$p < 0.001$; **$p < 0.01$; *$p < 0.05$; n.s. (no significance): $p > 0.05$; Student's *t*-test.

regions, but few studies have focused on the molecular analysis of this species. This legume grows rapidly and has a large biomass, with a well-developed root system (Nurfeta, 2010). However, it is unknown how its production could be regulated and improved via molecular biology. Abiotic stresses including cold and drought stress limit the distribution of *D. intortum*. Therefore, a better understanding of signal transduction during these processes would lay the foundation for further optimizing stress tolerance in this forage crop (Kulkarni et al., 2018). For instance, heterologous expression of *OsSIZ1*, a rice SUMO E3 ligase, enhances abiotic stress tolerance in transgenic creeping bentgrass (Li et al., 2013). Our study represents the first characterization of the molecular role of a SUMO ligase from *D. intortum* and provides hints about its roles in development and stress responses. These results provide a basis for improving the productivity and stress tolerance of this forage crop. In the future, it would be valuable to modulate the expression of *DiMMS21* in *D. intortum* and examine its effects on stress tolerance and growth in this forage legume.

5. Conclusion

We isolated the cDNA of an MMS21 homolog from *D. intortum* and measured its gene expression profile, subcellular localization, and SUMO ligase activity. *DiMMS21* overexpression completely rescued the developmental defects of an Arabidopsis *mms21* mutant but not its ABA sensitivity, thus uncovering similarities and differences between these MMS21 homologs. This study increases our understanding of the roles of SUMOylation in the development and stress responses of forage legumes.

Author contribution statement

Jianbin Lai and Chengwei Yang designed the experiments; Xuan Zhou conducted most of experiments; Jinju Du and Yiyang Liu provided technological supports; Jianbin Lai and Xuan Zhou analyzed data and wrote the manuscript.

Conflicts of interest

The authors declare that they have no competing interests.

Acknowledgements

We thank the Arabidopsis Biological Resource Center for the seeds and thank Professor Andreas Bachmair for the SUMO E1 plasmid used in this study. This work was supported by the National Natural Science Foundation of China (31871222, 31670286, 31771504), the Natural Science Foundation of Guangdong (2018B030308002), the Program for Changjiang Scholars, the Guangdong YangFan Innovative and Entrepreneurial Research Team Project (2015YT02H032) and the Guangzhou Scientific and Technological Program (201607010377).

Appendix A. Supplementary data

Supplementary data related to this article can be found at https://doi.org/10.1016/j.plaphy.2019.06.003.

References

Augustine, R.C., Vierstra, R.D., 2018. SUMOylation: re-wiring the plant nucleus during stress and development. Curr. Opin. Plant Biol. 45, 143–154.

Budhiraja, R., Hermkes, R., Muller, S., Schmidt, J., Colby, T., Panigrahi, K., Coupland, G., Bachmair, A., 2009. Substrates related to chromatin and to RNA-dependent processes are modified by Arabidopsis SUMO isoforms that differ in a conserved residue with influence on desumoylation. Plant Physiol. 149, 1529–1540.

Cai, B., Kong, X., Zhong, C., Sun, S., Zhou, X.F., Jin, Y.H., Wang, Y., Li, X., Zhu, Z., Jin, J.B., 2017. SUMO E3 ligases GmSIZ1a and GmSIZ1b regulate vegetative growth in soybean. J. Integr. Plant Biol. 59, 2–14.

Castro, P.H., Tavares, R.M., Bejarano, E.R., Azevedo, H., 2012. SUMO, a heavy weight player in plant abiotic stress responses. Cell. Mol. Life Sci. 69, 3269–3283.

Castro, P.H., Verde, N., Lourenco, T., Magalhaes, A.P., Tavares, R.M., Bejarano, E.R., Azevedo, H., 2015. SIZ1-dependent post-translational modification by SUMO modulates sugar signaling and metabolism in *Arabidopsis thaliana*. Plant Cell Physiol. 56, 2297–2311.

Castro, P.H., Santos, M.A., Freitas, S., Cana-Quijada, P., Lourenco, T., Rodrigues, M.A.A., Fonseca, F., Ruiz-Albert, J., Azevedo, J.E., Tavares, R.M., Castillo, A.G., Bejarano, E.R., Azevedo, H., 2018. Arabidopsis thaliana SPF1 and SPF2 are nuclear-located ULP2-like SUMO proteases that act downstream of SIZ1 in plant development. J. Exp. Bot. 69, 4633–4649.

Catala, R., Ouyang, J., Abreu, I.A., Hu, Y., Seo, H., Zhang, X., Chua, N.H., 2007. The Arabidopsis E3 SUMO ligase SIZ1 regulates plant growth and drought responses. Plant Cell 19, 2952–2966.

Clough, S.J., Bent, A.F., 1998. Floral dip: a simplified method for Agrobacterium-mediated transformation of *Arabidopsis thaliana*. Plant J. 16, 735–743.

Debela, E., Tolera, A., Eik, L.O., Salte, R., 2012. Condensed tannins from *Sesbania sesban* and *Desmodium intortum* as a means of *Haemonchus contortus* control in goats. Trop. Anim. Health Prod. 44, 1939–1944.

Duan, X., Sarangi, P., Liu, X., Rangi, G.K., Zhao, X., Ye, H., 2009. Structural and functional insights into the roles of the Mms21 subunit of the Smc5/6 complex. Mol. Cell 35, 657–668.

Elrouby, N., 2017. Regulation of plant cellular and organismal development by SUMO. Adv. Exp. Med. Biol. 963, 227–247.

Gasteiger, E., Gattiker, A., Hoogland, C., Ivanyi, I., Appel, R.D., Bairoch, A., 2003. ExPASy: the proteomics server for in-depth protein knowledge and analysis. Nucleic Acids Res. 31, 3784–3788.

Hay, R.T., 2013. Decoding the SUMO signal. Biochem. Soc. Trans. 41, 463–473.

Huang, L., Yang, S., Zhang, S., Liu, M., Lai, J., Qi, Y., Shi, S., Wang, J., Wang, Y., Xie, Q., Yang, C., 2009. The Arabidopsis SUMO E3 ligase AtMMS21, a homologue of NSE2/MMS21, regulates cell proliferation in the root. Plant J. 60, 666–678.

Ishida, T., Fujiwara, S., Miura, K., Stacey, N., Yoshimura, M., Schneider, K., Adachi, S., Minamisawa, K., Umeda, M., Sugimoto, K., 2009. SUMO E3 ligase HIGH PLOIDY2 regulates endocycle onset and meristem maintenance in Arabidopsis. Plant Cell 21, 2284–2297.

Ishida, T., Yoshimura, M., Miura, K., Sugimoto, K., 2012. MMS21/HPY2 and SIZ1, two Arabidopsis SUMO E3 ligases, have distinct functions in development. PLoS One 7, e46897.

Kelley, L.A., Mezulis, S., Yates, C.M., Wass, M.N., Sternberg, M.J., 2015. The Phyre2 web portal for protein modeling, prediction and analysis. Nat. Protoc. 10, 845–858.

Kerscher, O., Felberbaum, R., Hochstrasser, M., 2006. Modification of proteins by ubiquitin and ubiquitin-like proteins. Annu. Rev. Cell Dev. Biol. 22, 159–180.

Kulkarni, K.P., Tayade, R., Asekova, S., Song, J.T., Shannon, J.G., Lee, J.D., 2018. Harnessing the potential of forage legumes, alfalfa, soybean, and cowpea for sustainable agriculture and global food security. Front. Plant Sci. 9, 1314.

Li, Z., Hu, Q., Zhou, M., Vandenbrink, J., Li, D., Menchyk, N., Reighard, S., Norris, A., Liu, H., Sun, D., Luo, H., 2013. Heterologous expression of OsSIZ1, a rice SUMO E3 ligase, enhances broad abiotic stress tolerance in transgenic creeping bentgrass. Plant Biotechnol. J. 11, 432–445.

Liu, M., Shi, S., Zhang, S., Xu, P., Lai, J., Liu, Y., Yuan, D., Wang, Y., Du, J., Yang, C., 2014. SUMO E3 ligase AtMMS21 is required for normal meiosis and gametophyte development in Arabidopsis. BMC Plant Biol. 14, 153.

Liu, F., Wang, X., Su, M., Yu, M., Zhang, S., Lai, J., Yang, C., Wang, Y., 2015. Functional characterization of DnSIZ1, a SIZ/PIAS-type SUMO E3 ligase from Dendrobium. BMC Plant Biol. 15, 225.

Liu, Y., Lai, J., Yu, M., Wang, F., Zhang, J., Jiang, J., Hu, H., Wu, Q., Lu, G., Xu, P., Yang, C., 2016. The Arabidopsis SUMO E3 ligase AtMMS21 dissociates the E2Fa/DPa complex in cell cycle regulation. Plant Cell 28, 2225–2237.

Midega, C.A.O., Wasonga, C.J., Hooper, A.M., Pickett, J.A., Khan, Z.R., 2017. Drought-tolerant Desmodium species effectively suppress parasitic striga weed and improve cereal grain yields in western Kenya. Crop Protect. 98, 94–101.

Miller, M.J., Barrett-Wilt, G.A., Hua, Z., Vierstra, R.D., 2010. Proteomic analyses identify a diverse array of nuclear processes affected by small ubiquitin-like modifier conjugation in Arabidopsis. Proc. Natl. Acad. Sci. U.S.A. 107, 16512–16517.

Miller, M.J., Scalf, M., Rytz, T.C., Hubler, S.L., Smith, L.M., Vierstra, R.D., 2013. Quantitative proteomics reveals factors regulating RNA biology as dynamic targets of stress-induced SUMOylation in Arabidopsis. Mol. Cell. Proteom. 12, 449–463.

Miura, K., Rus, A., Sharkhuu, A., Yokoi, S., Karthikeyan, A.S., Raghothama, K.G., Baek, D., Koo, Y.D., Jin, J.B., Bressan, R.A., Yun, D.J., Hasegawa, P.M., 2005. The Arabidopsis SUMO E3 ligase SIZ1 controls phosphate deficiency responses. Proc. Natl. Acad. Sci. U.S.A. 102, 7760–7765.

Miura, K., Lee, J., Jin, J.B., Yoo, C.Y., Miura, T., Hasegawa, P.M., 2009. Sumoylation of ABI5 by the Arabidopsis SUMO E3 ligase SIZ1 negatively regulates abscisic acid signaling. Proc. Natl. Acad. Sci. U.S.A. 106, 5418–5423.

Miura, K., Lee, J., Miura, T., Hasegawa, P.M., 2010. SIZ1 controls cell growth and plant development in Arabidopsis through salicylic acid. Plant Cell Physiol. 51, 103–113.

Murtas, G., Reeves, P.H., Fu, Y.F., Bancroft, I., Dean, C., Coupland, G., 2003. A nuclear protease required for flowering-time regulation in Arabidopsis reduces the abundance of SMALL UBIQUITIN-RELATED MODIFIER conjugates. Plant Cell 15, 2308–2319.

Nurfeta, A., 2010. Digestibility and nitrogen utilization in sheep fed enset (Ensete ventricosum) pseudostem or corm and graded levels of *Desmodium intortum* hay to wheat straw-based diets. J. Anim. Physiol. Anim. Nutr. 94, 773–779.

Nurfeta, A., Tolera, A., Eik, L.O., Sundstol, F., 2009. Feeding value of enset (*Ensete ventricosum*), *Desmodium intortum* hay and untreated or urea and calcium oxide treated wheat straw for sheep. J. Anim. Physiol. Anim. Nutr. 93, 94–104.

Okada, S., Nagabuchi, M., Takamura, Y., Nakagawa, T., Shinmyozu, K., Nakayama, J., Tanaka, K., 2009. Reconstitution of *Arabidopsis thaliana* SUMO pathways in *E. coli*: functional evaluation of SUMO machinery proteins and mapping of SUMOylation sites by mass spectrometry. Plant Cell Physiol. 50, 1049–1061.

Park, H.J., Yun, D.J., 2013. New insights into the role of the small ubiquitin-like modifier (SUMO) in plants. Int. Rev. Cell Mol. Biol. 300, 161–209.

Park, H.C., Kim, H., Koo, S.C., Park, H.J., Cheong, M.S., Hong, H., Baek, D., Chung, W.S., Kim, D.H., Bressan, R.A., Lee, S.Y., Bohnert, H.J., Yun, D.J., 2010. Functional characterization of the SIZ/PIAS-type SUMO E3 ligases, OsSIZ1 and OsSIZ2 in rice. Plant Cell Environ. 33, 1923–1934.

Rytz, T.C., Miller, M.J., McLoughlin, F., Augustine, R.C., Marshall, R.S., Juan, Y.T., Charng, Y.Y., Scalf, M., Smith, L.M., Vierstra, R.D., 2018. SUMOylome profiling reveals a diverse array of nuclear targets modified by the SUMO ligase SIZ1 during heat stress. Plant Cell 30, 1077–1099.

Saracco, S.A., Miller, M.J., Kurepa, J., Vierstra, R.D., 2007. Genetic analysis of SUMOylation in Arabidopsis: conjugation of SUMO1 and SUMO2 to nuclear proteins is essential. Plant Physiol. 145, 119–134.

Seeler, J.S., Dejean, A., 2003. Nuclear and unclear functions of SUMO. Nat. Rev. Mol. Cell Biol. 4, 690–699.

Sievers, F., Wilm, A., Dineen, D., Gibson, T.J., Karplus, K., Li, W., Lopez, R., McWilliam, H., Remmert, M., Soding, J., Thompson, J.D., Higgins, D.G., 2011. Fast, scalable generation of high-quality protein multiple sequence alignments using Clustal Omega. Mol. Syst. Biol. 7, 539.

Tamura, K., Peterson, D., Peterson, N., Stecher, G., Nei, M., Kumar, S., 2011. MEGA5: molecular evolutionary genetics analysis using maximum likelihood, evolutionary distance, and maximum parsimony methods. Mol. Biol. Evol. 28, 2731–2739.

Truernit, E., Haseloff, J., 2008. A simple way to identify non-viable cells within living plant tissue using confocal microscopy. Plant Methods 4, 15.

van den Burg, H.A., Takken, F.L., 2010. SUMO-, MAPK-, and resistance protein-signaling converge at transcription complexes that regulate plant innate immunity. Plant Signal. Behav. 5, 1597–1601.

Wilkinson, K.A., Henley, J.M., 2010. Mechanisms, regulation and consequences of protein SUMOylation. Biochem. J. 428, 133–145.

Xu, P., Yuan, D., Liu, M., Li, C., Liu, Y., Zhang, S., Yao, N., Yang, C., 2013. AtMMS21, an SMC5/6 complex subunit, is involved in stem cell niche maintenance and DNA damage responses in Arabidopsis roots. Plant Physiol. 161, 1755–1768.

Yang, Y., Yu, X., Song, L., An, C., 2011. ABI4 activates DGAT1 expression in Arabidopsis seedlings during nitrogen deficiency. Plant Physiol. 156, 873–883.

Yoo, S.D., Cho, Y.H., Sheen, J., 2007. Arabidopsis mesophyll protoplasts: a versatile cell system for transient gene expression analysis. Nat. Protoc. 2, 1565–1572.

Yu, M., Meng, B., Wang, F., He, Z., Hu, R., Du, J., Lai, J., Yang, C., 2019. A SUMO ligase AtMMS21 regulates activity of the 26S proteasome in root development. Plant Sci. 280, 314–320.

Yuan, D., Lai, J., Xu, P., Zhang, S., Zhang, J., Li, C., Wang, Y., Du, J., Liu, Y., Yang, C., 2014. AtMMS21 regulates DNA damage response and homologous recombination repair in Arabidopsis. DNA Repair 21, 140–147.

Zhang, S., Qi, Y., Liu, M., Yang, C., 2013. SUMO E3 ligase AtMMS21 regulates drought tolerance in *Arabidopsis thaliana*. J. Integr. Plant Biol. 55, 83–95.

Zhang, R.F., Guo, Y., Li, Y.Y., Zhou, L.J., Hao, Y.J., You, C.X., 2016. Functional identification of MdSIZ1 as a SUMO E3 ligase in apple. J. Plant Physiol. 198, 69–80.

Zhang, J., Lai, J., Wang, F., Yang, S., He, Z., Jiang, J., Li, Q., Wu, Q., Liu, Y., Yu, M., Du, J., Xie, Q., Wu, K., Yang, C., 2017a. A SUMO ligase AtMMS21 regulates the stability of the chromatin remodeler BRAHMA in root development. Plant Physiol. 173, 1574–1582.

Zhang, S., Zhuang, K., Wang, S., Lv, J., Ma, N., Meng, Q., 2017b. A novel tomato SUMO E3 ligase, SlSIZ1, confers drought tolerance in transgenic tobacco. J. Integr. Plant Biol. 59, 102–117.